

Article

# Investigation of the Causes of Soft-Storey and Weak-Storey Formations in Low- and Mid-Rise RC Buildings in Türkiye

Hakan Ulutaş 

Department of Civil Engineering, Faculty of Engineering and Architecture, Burdur Mehmet Akif Ersoy University, Burdur 15030, Turkey; hulutas@mehmetakif.edu.tr; Tel.: +90-(248)-213-2746

**Abstract:** This study investigates the causes of soft-storey and weak-storey formations in low- and mid-rise RC (Reinforced Concrete) buildings in Türkiye. In the first phase of the study, 96 model buildings were designated for the examination of soft-storey irregularity when the ground floors are used for commercial purposes and the upper floors for residential use. The ground floor heights that would cause soft-storey irregularity in each of the selected buildings were determined according to the formulas given in the Türkiye Building Earthquake Code (TBEC) and the American Society of Civil Engineers Standard (ASCE). It was found that the ground floor heights obtained according to ASCE are usable in practice, whereas those obtained according to the TBEC, particularly for buildings over three storeys, are excessively high for practical use. This indicates that, even if the buildings in Türkiye are designed with very high ground floor heights, they do not have soft-storey irregularities, according to the TBEC, but soft-storey formation may occur in these buildings due to the high ground floor height as a result of the effects of earthquakes. Instead of the soft-storey irregularity coefficient limit value ( $n_{ki} > 2$ ) found in the TBEC, this study proposes a new limit value to prevent the design of buildings with very high ground floors. In the second phase of the study, for the purpose of examining weak-storey irregularity, 105 model buildings differing in their infill wall layout, number of spans, span length, and number of storeys were selected. The weak-storey irregularity coefficients of each of these models were determined according to the TBEC. The results of the study revealed that buildings with no infill walls in one direction or with infill walls in only one of the exterior axes in one direction have a high risk of having weak storeys.

**Keywords:** ASCE; damage; irregularity; soft-storey; TBEC; weak-storey



**Citation:** Ulutaş, H. Investigation of the Causes of Soft-Storey and Weak-Storey Formations in Low- and Mid-Rise RC Buildings in Türkiye. *Buildings* **2024**, *14*, 1308. <https://doi.org/10.3390/buildings14051308>

Academic Editor: Harry Far

Received: 27 February 2024

Revised: 22 April 2024

Accepted: 30 April 2024

Published: 6 May 2024



**Copyright:** © 2024 by the author. Licensee MDPI, Basel, Switzerland. This article is an open access article distributed under the terms and conditions of the Creative Commons Attribution (CC BY) license (<https://creativecommons.org/licenses/by/4.0/>).

## 1. Introduction

Türkiye is situated across active earthquake fault zones, including the North Anatolian Fault, the East Anatolian Fault, and the West Anatolian Fault Zone, which have the potential to cause devastating earthquakes. The North Anatolian Fault and the East Anatolian Fault are among the most seismically active faults in the world with the shortest return periods [1–3]. In recent years, earthquakes caused by these faults have led to the deaths and injuries of thousands of people and the collapse or damage of numerous buildings [4–8]. Information about major earthquakes that occurred in Türkiye in the last 25 years is presented in Table 1.

Numerous studies have been conducted to investigate the causes of damage to buildings following earthquakes [2,10–42]. Researchers have identified the primary causes of building damage as ground failures, soil liquefaction, poor concrete strength quality, unribbed reinforcement steel, poor detailing in beam–column joints, strong beam–weak columns, soft or weak storeys, inadequate transverse reinforcement, the existence of short lap splices and incorrect end hook angles, short columns, weak walls, inadequate safe distance between buildings, unconfined gable walls, concrete slab failures, and insulation materials. One of the main reasons for the collapse or damage of reinforced concrete structures during earthquakes, both in Türkiye and globally, is the critical storey exhibiting

soft or weak-storey behaviour [8,43–45]. Soft-storey formation is caused by the difference in stiffness between neighbouring storeys. The difference in stiffness between neighbouring storeys causes different amounts of displacement in the storeys due to lateral loads. If the ratio of drift between the storeys is too high, the building cannot cope with lateral forces. Weak-storey formation is caused by the difference in strength between neighbouring storeys. The strength of a storey is obtained by summing the cross-sectional areas of the load-bearing elements. According to TBEC, 15% of the cross-sectional area of the infill walls is taken into account in the calculation of weak-storey irregularity. Since the cross-sectional areas of columns and shear walls generally do not change between storeys in low- and mid-rise RC buildings, the difference in the amount of infill walls between neighbouring storeys may cause weak-storey irregularity in such buildings. It is necessary to avoid sudden changes in lateral stiffness and strength, since a large difference in stiffness or strength between storeys will prevent the building from moving as a whole [8,46,47]. Kirac et al. [41] reported that 78% of a group of 300,000 buildings in Türkiye had soft- or weak-storey configurations and that 725 out of 1215 RC buildings were damaged due to weak-storey configurations during the 1999 İzmit earthquake. Some of the damages or collapses caused by soft or weak-storey formations due to major earthquakes in Türkiye in the last 25 years are shown in Figure 1.

**Table 1.** Major earthquakes in Türkiye in the last 25 years [9].

Earthquake	Magnitude ( $M_w$ )	Impacts of the Earthquake
17 August 1999, Gölcük Earthquake	7.4	A total of 17,480 people died, and 23,781 were injured. In addition, 35,180 residences and 5,770 workplaces collapsed or were severely damaged.
1 May 2003, Bingöl Earthquake	6.4	A total of 176 people died, and 521 were injured. In addition, 1,351 buildings were collapsed or severely damaged.
23 October 2011, Van Earthquake	7.2	A total of 644 people died, and 1,966 were injured. In addition, 2,262 buildings collapsed; 5,739 buildings were damaged and became uninhabitable.
24 January 2020, Elazığ-Sivrice Earthquake	6.8	A total of 41 people died, and 1,607 were injured. In addition, 547 buildings collapsed, and 6,270 buildings were severely damaged.
30 October 2020, İzmir Earthquake	6.9	A total of 119 people died in Türkiye and Greece, and 1,053 were injured. In addition, 124 buildings were severely damaged or collapsed.
6 February 2023, Kahramanmaraş Earthquakes	7.7 and 7.6	According to official figures, at least 50,783 people in Türkiye and 8,476 in Syria died, and over 122,000 were injured. In addition, 227,027 buildings were identified as having collapsed or having been severely damaged.

In Türkiye, most buildings constructed along main streets are likely to exhibit soft or weak storey behaviour in case of an earthquake. Because the ground floors of these buildings are generally used for commercial purposes, glass windows are preferred instead of infill walls, and the ground floor heights are made to be higher than the heights of the upper floors. Heavy masonry infill walls often start right above the soft storey. In addition, since there are not enough infill walls on this floor in buildings whose basements are used as parking, and multi-storey parking generally has wide retail space or floors with multiple windows, these buildings are at high risk of weak-storey formation [46,52].

Soft- and weak-storey formations are important structural irregularities that should be avoided for capacity design reasons [51]. A soft storey is a relatively flexible storey where the relative horizontal displacement of any storey is much greater than that of the storey above or below it. These floors can be dangerous in earthquakes because they cannot cope with the lateral forces due to the vibrations occurring in the building during the earthquake. Soft-storey formations lead to a significant increase in deformation demands and cause the load of energy dissipation to be placed on the columns in this storey. Buildings with soft ground floor concentrate large drift ratio demands on the first floor and low demands on the upper floors, resulting in severe damage to or the collapse of the building [46,53–55]. Additionally, the presence of poor column–beam connections and weak columns are primary causes for the development of soft-storey mechanisms [50].

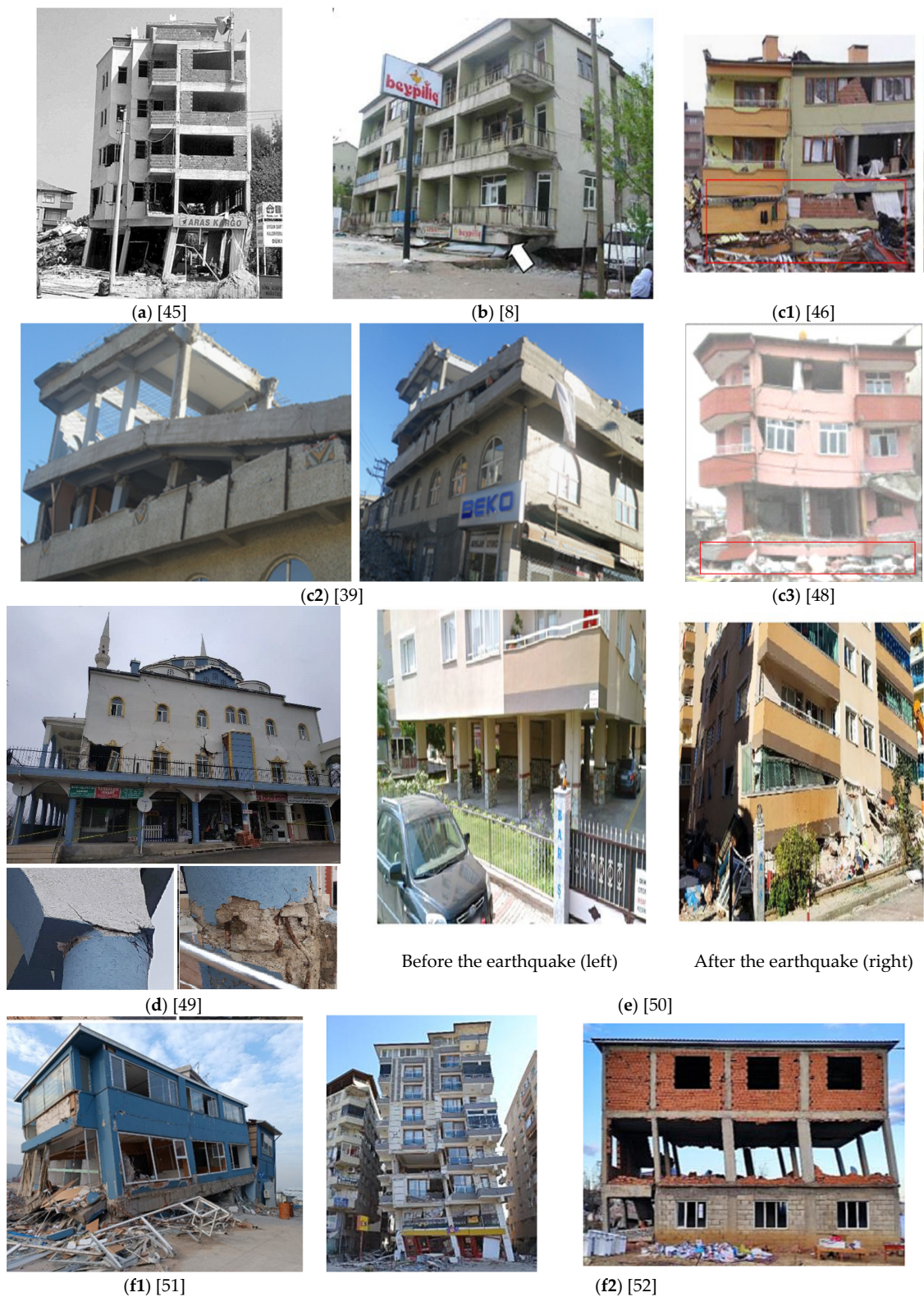


**Figure 1.** Damages and collapses observed in some buildings with weak- and/or soft-storey formation: (a) 17 August 1999 Kocaeli earthquake [45]; (b) 1 May 2003 Bingöl earthquake [8]; (c1–c3) 23 October 2011 Van earthquake [39,46,48]; (d) 24 January 2020 Sivrice earthquake [49]; (e) 30 October 2020 izmir Earthquake [50]; (f1,f2) 6 February 2023 Kahramanmaraş earthquake [51,52].

This study aims to contribute to preventing damage to Turkish buildings due to soft or weak-storey formations. In the first part of the study, 96 different models were created

for the examination of soft-storey irregularity, with the ground floor used for commercial purposes and the upper floors used for residential purposes. The minimum ground floor heights that would cause soft-storey formation in each model were calculated according to the TBEC [56] and ASCE [57] regulations, and the results were compared. At the end of this part of the study, a proposal is made for a new soft-storey irregularity coefficient limit value ( $n_{ki} > 2$ ) for the TBEC. In the second part of the study, 105 buildings with different numbers of spans, span lengths, number of storeys, and infill wall layouts were selected. The weak-storey irregularity coefficients for each model were calculated. According to the ground floor heights obtained in the first part of the study and the weak-storey irregularity coefficients obtained in the second part, it was interpreted the reasons why buildings in Türkiye were damaged due to soft- or weak-storey formations. It is believed that considering the proposed soft-storey irregularity limit value and recommendations regarding infill wall layout will contribute to reducing the number of buildings damaged due to such formations.

## 2. Soft-Storey and Weak-Storey in ASCE 7-22 and TBEC-2018 Code Provision

### 2.1. Soft-Storey Irregularity

According to the TBEC, the soft-storey irregularity coefficient ( $n_{ki}$ ) should be calculated to check the soft-storey irregularity of a reinforced concrete building. The soft-storey irregularity coefficient is obtained by dividing the average relative storey drift ratio at any  $i$ -th storey by the average relative storey drift ratio at an upper or a lower storey for either of two orthogonal directions. If the soft-storey irregularity coefficient ( $n_{ki}$ ) exceeds 2.0 on any of the floors, it implies that there is soft-storey irregularity in the building. The equation for the soft-storey irregularity coefficient ( $n_{ki}$ ) of the  $x$ -direction is shown in Equation (1).

$$n_{ki} = \frac{(\Delta_i^{(X)}/h_i)_{avg}}{(\Delta_{i+1}^{(X)}/h_{i+1})_{avg}} > 2 \text{ or } n_{ki} = \frac{(\Delta_i^{(X)}/h_i)_{avg}}{(\Delta_{i-1}^{(X)}/h_{i-1})_{avg}} > 2 \quad (1)$$

Here,  $h_i$  represents the storey height of the  $i$ -th floor, while  $\Delta_i^{(X)}_{(avg)}$  denotes the average relative storey drift of the  $i$ -th floor, which is obtained using Equation (2).

$$\Delta_i^{(X)}_{(avg)} = 0.5 * ((\Delta_i^{(X)})_{max} + (\Delta_i^{(X)})_{min}) \quad (2)$$

In Equation (2),  $\Delta_i^{(X)}_{(max)}$  and  $\Delta_i^{(X)}_{(min)}$  represent the maximum and minimum relative storey drifts of the  $i$ -th floor, respectively. Relative storey drifts are calculated using Equation (3).

$$\Delta_i^{(X)} = u_i^{(X)} - u_{(i-1)}^{(X)} \quad (3)$$

In Equation (3),  $u_i^{(X)}$  denotes the total displacement of the  $i$ -th floor. The terms given in Equations (2) and (3) are illustrated in Figure 2.

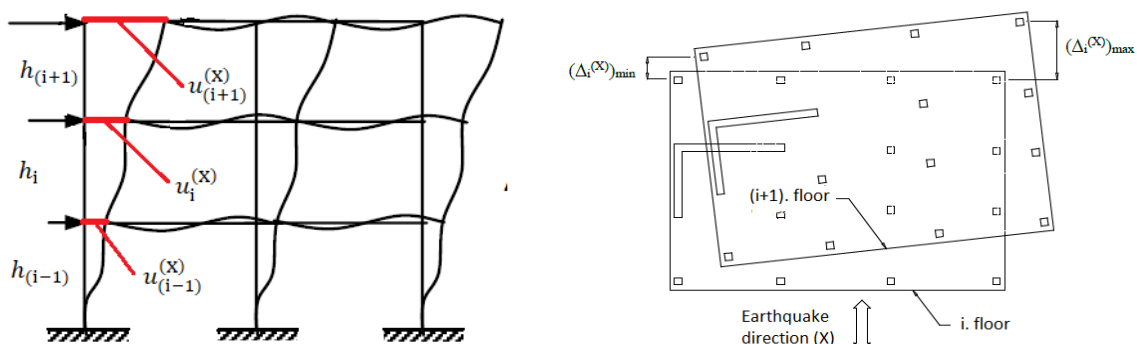


Figure 2. Obtaining the relative storey drift.

In order to calculate the soft-storey irregularity coefficient ( $n_{ki}$ ) the building is solved with the equivalent lateral force method, which is one of the linear analysis methods. The soft-storey irregularity coefficient is calculated by using the relative storey drifts obtained from this analysis in Equation (1).

According to ASCE, the soft-storey irregularity of a reinforced concrete building is checked by looking at the lateral stiffness of the storeys ( $K_i$ ). In this regulation, two types of irregularity conditions are defined: Stiffness-Soft Storey Irregularity and Stiffness-Extreme Soft Storey Irregularity.

Stiffness-Soft Storey Irregularity is defined as existing where there is a storey in which the lateral stiffness is less than 70% of that in the storey above or, where there are at least three storeys above, less than 80% of the average stiffness of the three storeys above (Equation (4)).

$$K_i < 0.7K_{i+1} \text{ or } K_i < \frac{0.8}{3}(K_{i+1} + K_{i+2} + K_{i+3}) \quad (4)$$

Stiffness-Extreme Soft Storey Irregularity is defined as existing where there is a storey in which the lateral stiffness is less than 60% of that in the storey above or, where there are at least three storeys above, less than 70% of the average stiffness of the three storeys above (Equation (5)).

$$K_i < 0.6K_{i+1} \text{ or } K_i < \frac{0.7}{3}(K_{i+1} + K_{i+2} + K_{i+3}) \quad (5)$$

The lateral stiffness of the storeys is calculated using Equation (6).

$$K_i^{(X)} = \frac{V_i^{(X)}}{\delta_i^{(X)}} \quad (6)$$

Here,  $\delta_i^{(X)}$  represents the deflection at the level of the center of mass  $x$  of the  $i$ -th floor determined by an elastic analysis, while  $V_i^{(X)}$  is the storey shear force at level  $x$  of the  $i$ -th floor determined by an equivalent lateral force method.

The terms in Equations (4) and (5) are schematized in Figure 3.

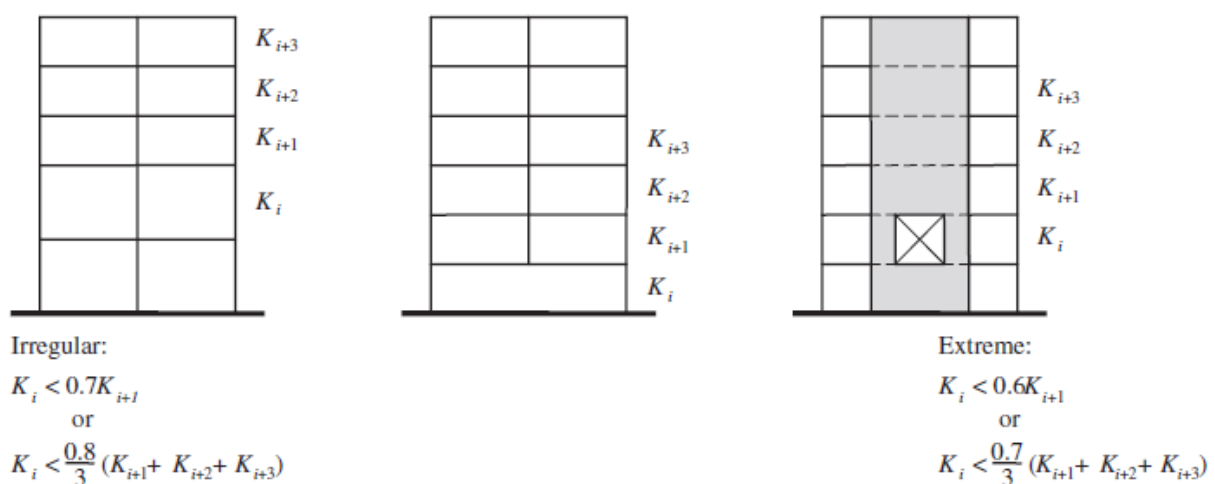


Figure 3. Soft-storey definition in ASCE [57].

## 2.2. Weak-Storey Irregularity

According to TBEC, the weak-storey irregularity coefficient ( $n_{ci}$ ) should be calculated to check the weak-storey irregularity of a reinforced concrete building. This coefficient is determined by comparing the total effective shear area of a given storey in one of the two orthogonal directions to that of the storey immediately above. The presence of weak-storey irregularity is confirmed if the calculated weak-storey irregularity coefficient ( $n_{ci}$ ) is less than 0.8 in any of these directions. The weak-storey irregularity coefficient ( $n_{ci}$ ) is derived as per Equation (7):

$$n_{ci} = \frac{(\sum A_e)_i}{(\sum A_e)_{i+1}} < 0.8 \quad (7)$$

In Equation (7), the term  $(\sum A_e)_i$  denotes the total effective shear area of the  $i$ -th storey, while  $(\sum A_e)_{i+1}$  represents the total effective shear area of the upper floor of the  $i$ -th floor. The total effective shear area can be obtained using Equation (8).

$$(\sum A_e)_i = (\sum A_w)_i + (\sum A_g)_i + (0.15 \sum A_k)_i \quad (8)$$

wherein:

$(\sum A_w)_i$ : The sum of column cross-section effective body areas at any floor ( $m^2$ );

$(\sum A_g)_i$ : The sum of the cross-sectional areas of shear walls parallel to the earthquake direction considered at any floor ( $m^2$ );

$(\sum A_k)_i$ : The sum of infill wall areas parallel to the considered earthquake direction at any floor ( $m^2$ ).

The material from which the infill walls are made does not change the effective shear area. In order for a wall to be evaluated as an infill wall, it must be constructed between the structural system elements, and other than that, it does not need to have specific specifications, such as the minimum thickness for infill walls.

In order to calculate the coefficient of weak-storey irregularity ( $n_{ci}$ ), the cross-sectional areas of columns, shear walls, and infill walls in each storey are calculated. The cross-sectional areas obtained are used in Equation (8) to obtain the effective shear area of the storeys. The effective shear areas obtained for all storey levels are used in Equation (7) to obtain the weak-storey irregularity coefficient.

According to the ASCE, the weak-storey irregularity of a reinforced concrete building is checked by looking at the lateral strength of the floors ( $Str_i$ ). In this regulation, two types of irregularity conditions are defined: Discontinuity in Lateral Strength-Weak Storey Irregularity and Discontinuity in Lateral Strength-Extreme Weak Storey Irregularity.

Discontinuity in Lateral Strength-Weak Storey Irregularity is defined as existing where the storey lateral strength is less than that in the storey above. The storey lateral strength is the total lateral strength of all of the seismic force-resisting system elements resisting the storey shear for the direction under consideration (Equation (9)).

$$Str_i < 1Str_{i+1} \quad (9)$$

Discontinuity in Lateral Strength-Extreme Weak Storey Irregularity is defined as existing where the storey lateral strength is less than 65% of that in the storey above. The storey lateral strength is the total lateral strength of all of the seismic force-resisting system elements resisting the storey shear for the direction under consideration (Equation (10)).

$$Str_i < 0.65Str_{i+1} \quad (10)$$

In Equations (9) and (10),  $\sum Str_i$  represents the total area of vertical structural elements to determine the strength of the storey.  $\sum Str_i$  corresponds to  $(\sum A_e)$  in Equation (8), and the sum of the infill wall areas is not used in the calculation of  $\sum Str_i$ .

The details and terminologies outlined in Equations (9) and (10) are illustrated in Figure 4.

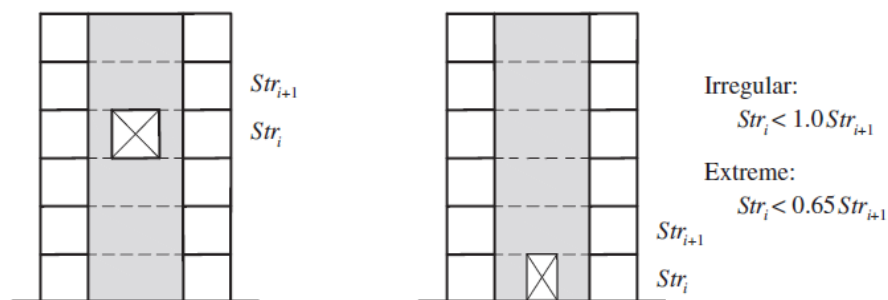


Figure 4. Weak-storey definition in ASCE [57].

### 3. Structural Models and Analysis Models

#### 3.1. Investigation of Soft-Storey Irregularity

The study encompasses eight types of formwork plans with commercial ground floors and residential upper floors. The characteristics of these buildings are presented in Table 2, and their formwork plans and 3D model illustrations are shown in Figure 5.

Table 2. Characteristics of the selected formwork plans.

FP1-O	FP1-CO	FP1-MF	FP1-SW
It represents buildings with a regular axis layout.	It is the version of the FP1-O formwork plan with a closed overhang.	It is the version of the FP1-O formwork plan with a mezzanine floor.	It is the version of the FP1-O formwork plan with an added reinforced concrete shear wall in the y-direction. It has torsional irregularity.
FP2-O	FP2-CO	FP2-MF	FP2-SW
It represents buildings with an irregular axis layout.	It is the version of the FP2-O formwork plan with a closed overhang.	It is the version of the FP2-O formwork plan with a mezzanine floor.	It is the version of the FP2-O formwork plan with an added reinforced concrete shear wall in the y-direction. It has torsional irregularity.

In all models, the beam widths are 25 cm, the heights are 50 cm, the floor dead load ( $g$ ) is 4.5 kN/m<sup>2</sup>, and the live load ( $q$ ) is 2 kN/m<sup>2</sup>. Variations in concrete class, soil type, and seismic parameters do not affect the soft-storey irregularity coefficient because changes in these parameters alter the amount of relative drift or lateral stiffness between floors in the same proportion [58]. In each formwork plan, two types of column layouts were made to also examine the effect of column direction on soft-storey irregularity. In the Type 1 column layout, all columns face the x-direction (the long dimension of the column section is in the x-direction), while in the Type 2 column layout, the number of columns facing the x and y-directions is equal. The short dimension of the column sections is 30 cm, and the long dimension is selected as given in Table 3, depending on the number of storeys. In order to be able to compare the models among themselves, the same values were selected for all models depending on the number of storeys. The selected column sections are commonly used dimensions depending on the number of storeys.

Table 3. Long direction dimensions of column sections depending on the number of storeys.

Number of Storeys	Long Direction Dimensions of the Column Sections (cm)
2	45
3	50
4	55
5	60
6	65
7	70

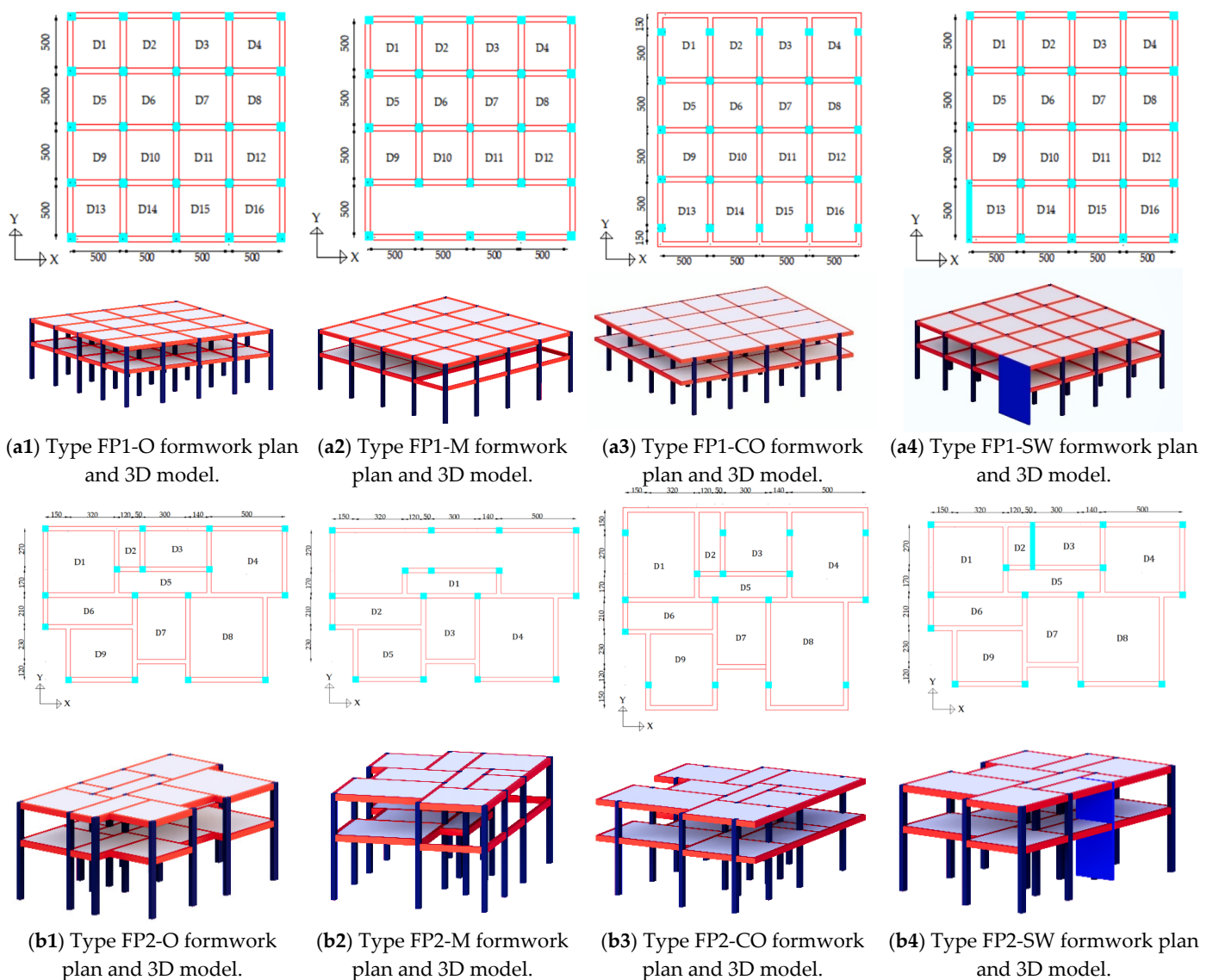


**Figure 5.** Selected formwork plans and 3D model illustrations (units in cm).

Since two types of column layouts are applied to each of the eight types of formwork plans, a total of 16 different formwork plan buildings were identified. Each of the sixteen types of formwork plans have been modelled to have two, three, four, five, six, and seven storeys. Thus, 96 building models were created. The height of the regular floors in the models is 3 m, and the height of the mezzanine floor is 2.5 m. One of the main reasons for soft-storey irregularity is the difference in height between the storeys. Because the difference in storey heights will cause the stiffness of the neighbouring storeys to be different. As a matter of fact, according to the ASCE, the soft-storey irregularity formula depends on the ratio of the stiffness of the neighbouring storeys (Equations (4) or (5)), while according to the TBEC, the soft-storey irregularity is calculated depending on the relative drift of the neighbouring storeys and the storey height (Equation (1)). Therefore, the ground floor heights of the model buildings were initially set at 3 m, and the soft-storey irregularity coefficient ( $n_{ki}$ ) was calculated on this basis. If  $n_{ki} < 2$ , the analysis was repeated by increasing the ground floor height by 5 cm until the soft-storey irregularity coefficient exceeded two. In the analyses, the  $\pm 5\%$  accidental eccentricity effect was considered to take into account the possible uncertainties in the stiffness and mass distribution of the carrying system. As a result, four  $n_{ki}$  values were considered in the analyses: two in each direction for each storey. In the analyses, the larger of the  $\eta_{ki}$  values obtained for the

x- and y-directions was taken into consideration as the soft-storey irregularity coefficient of the building. In other words, the analyses were repeated until any of the four  $n_{ki}$  values exceeded two. Thus, the minimum ground floor height ( $h_{gf}$ ) causing soft-storey irregularity in buildings according to the TBEC has been calculated for all models. The aim here is to evaluate how appropriate the ground floor heights obtained are for practice and to allow the models with different formwork plans to be compared with each other.

The ground floor height ( $h_{gf}$ ) obtained for each of the two types of column layouts depending on the number of storeys is presented in Figure 6.

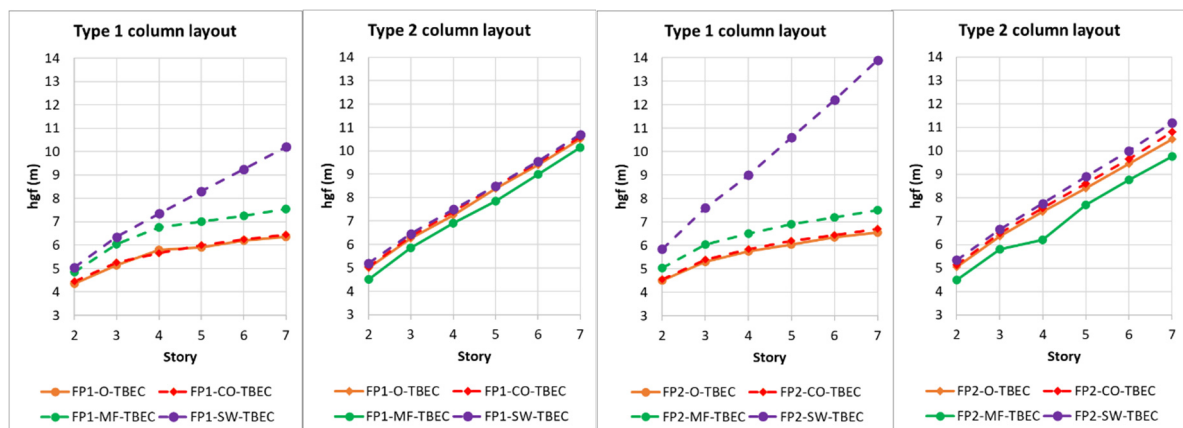


**Figure 6.** Ground floor heights ( $h_{gf}$ ) causing soft-storey irregularity according to TBEC, depending on the number of storeys.

Considering the results obtained according to the TBEC, for the Type 1 column layout, the presence of a shear wall in one direction or a mezzanine floor in the building causes soft-storey irregularities at higher ground floor heights than the original models (FP1-O or FP2-O). In other words, the presence of a shear wall in one direction or a mezzanine floor has reduced the risk of soft-storey irregularities. The closed overhang in the building did not change the results compared to the original models. However, for the Type 2 column layout, the presence of a mezzanine floor in the building caused soft-storey irregularities at lower ground floor heights than the original models (FP1-O or FP2-O). The presence of a shear wall in only one direction or a closed overhang in the building changed the  $h_{gf}$  values (ground floor heights causing soft-storey irregularities) only slightly compared to the original models (FP1-O or FP2-O). Therefore, it can be said that the presence of a mezzanine floor increases the risk of soft-storey irregularity, while the presence of a shear wall in only one direction or a closed overhang in the building has a limited impact on soft-storey irregularity. The results obtained according to the formulas in TBCE are far from the ground floor heights used in practice. Also, the presence of a mezzanine is not expected to reduce the risk of soft-storey irregularities.

The same model buildings were analysed according to ASCE, and the minimum ground floor height ( $h_{gf}$ ) that would cause soft-storey irregularity was obtained in all models (Figure 7). Unlike the TBEC, minimum ground floor heights ( $h_{gf}$ ) were determined by considering Equation (3) instead of Equation (1).

The results obtained according to the ASCE indicate that the presence of a mezzanine floor in buildings with both types of column layouts increases the risk of a soft storey, while the presence of a closed overhang almost does not alter the results at all. Additionally, it was found that the presence of a shear wall in one direction reduces the risk of a soft storey in Type 1 column layouts but does not change this risk in Type 2 column layouts. Here, it can be concluded that the effect of shear wall placement in one direction on soft-storey irregularity is limited in regular column layouts. The results obtained according to the ASCE are ground floor heights that can be used in practice. The results given by the soft-storey irregularity formulas in ASCE for different formwork plans are reasonable and expected.

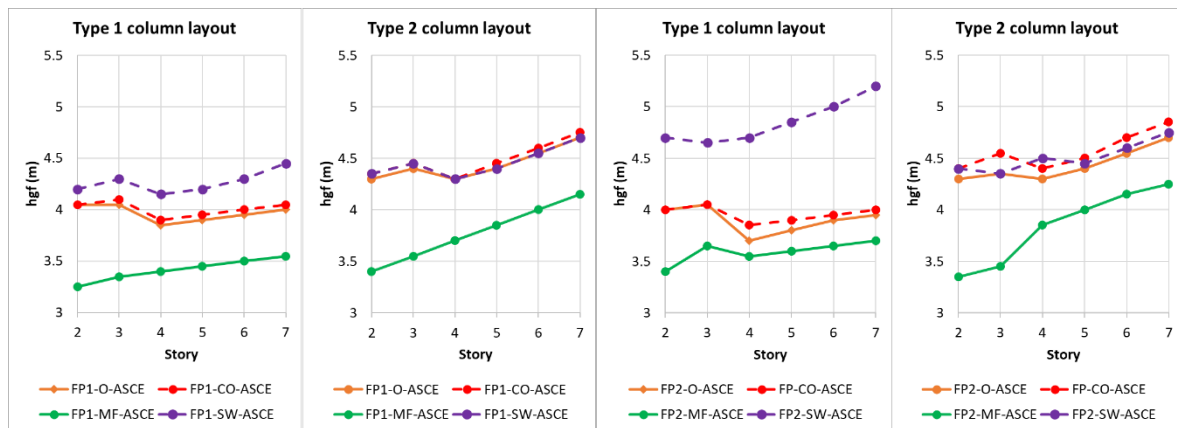


**Figure 7.** Ground floor heights causing soft-storey irregularity according to ASCE, depending on the number of storeys.

Figures 6 and 7 show that changes in the number of storeys do not significantly alter the results according to the ASCE, while according to the TBEC, the  $h_{gf}$  values increase more noticeably as the number of storeys increases. So that, according to TBEC, the ratio of the ground floor height causing a soft-storey irregularity in a seven-storey building to that in a two-storey building is on average 1.66 for the Type 1 column layout (average value obtained from eight typical formwork plans) and 2.1 for the Type 2 column layout.

For a comparison of the results obtained according to the TBEC and ASCE regulations, the  $h_{gf}$  values obtained according to both regulations are shown on the same graph (Figure 8).

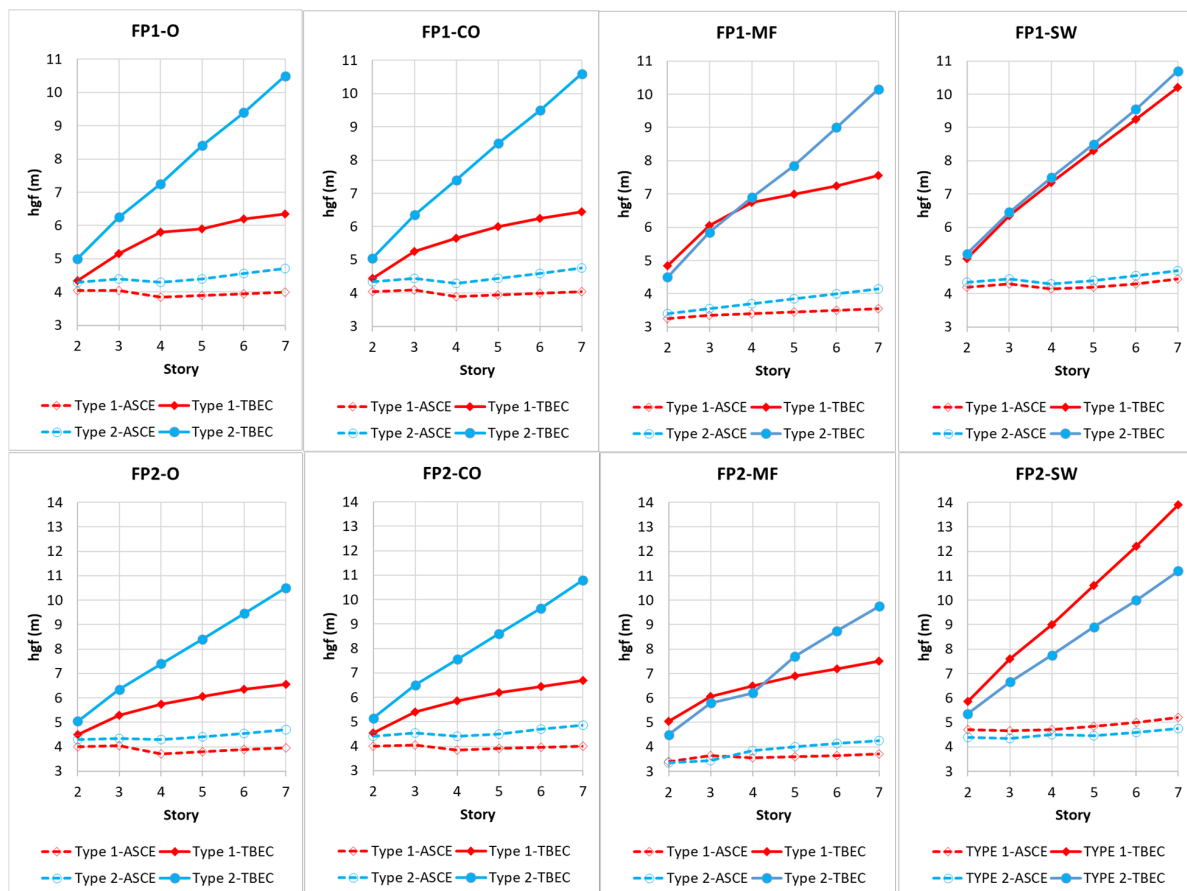


**Figure 8.** Comparison of  $h_{gf}$  results obtained according to TBEC and ASCE.

Figure 8 shows that there are significant differences between the results obtained according to the TBEC and ASCE regulations. The soft-storey irregularity formulas in the ASCE give more reasonable and consistent results than those in the TBEC. For a numerical comparison of the differences between the regulations, the  $h_{gf}$  values obtained with the TBEC were rationed to the values obtained according to the ASCE (Figure 9).

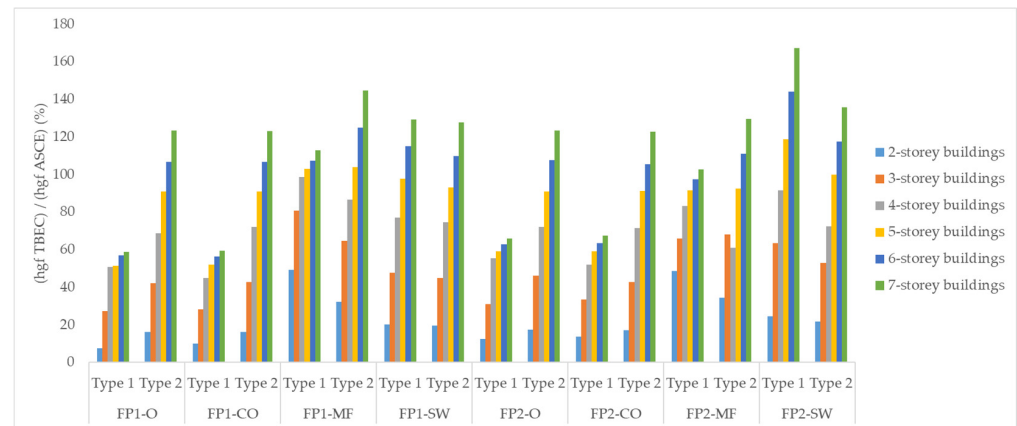


**Figure 9.**  $h_{gf}$  ratios obtained according to regulations, depending on the formwork plan and column layout.

Figure 9 shows that the difference in results obtained with the TBEC and ASCE regulations (ground floor heights causing soft-storey irregularity) increases as the number of storeys increases. The greatest difference among the regulations occurred in the FP2-SW formwork plan's Type 1 column layout, reaching 167%.

As seen in Figure 6, considering the results obtained according to the TBEC, the ground floor height ( $h_{gf}$ ) causing soft-storey irregularity in four-storey model buildings was obtained as at least 5.75 m for the Type 1 column layout (the smallest value obtained from eight types of formwork plans) and at least 6.2 m for the Type 2 column layout. As the number of storeys increases, these values also increase. These values are not the ground floor heights seen in practice. As seen in Figure 7, the ground floor heights ( $h_{gf}$ ) obtained according to the ASCE are between 3.25 and 5.2 m, and these values are the ground floor heights frequently encountered in practice. Therefore, the ground floor height of each model building was chosen as the minimum ground floor height ( $h_{gf}$ ) that causes soft-storey irregularity in that building according to the ASCE, and the soft-storey irregularity coefficients of the buildings were recalculated according to the formula given in the TBEC (see Figure 10). The aim was to determine the range within which the obtained  $n_{ki}$  values fall.

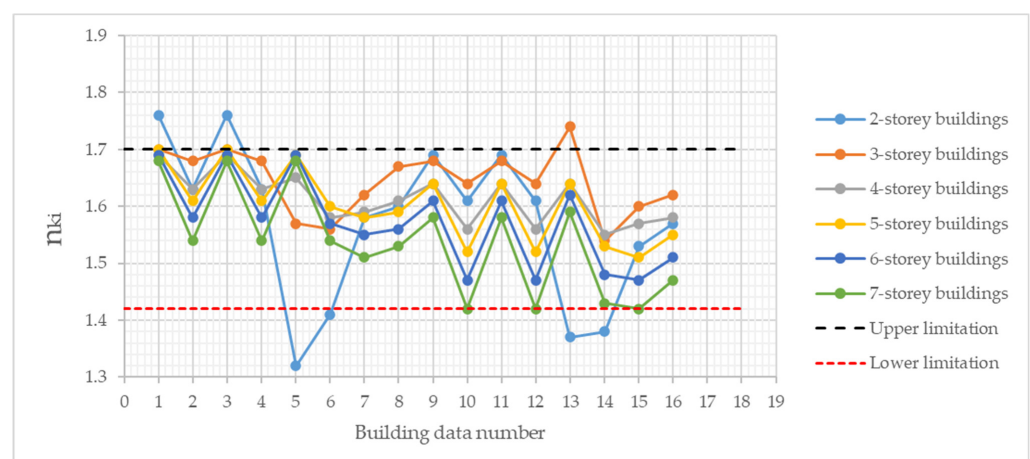


**Figure 10.** The  $n_{ki}$  values determined using the ( $h_{gf}$ ) values obtained according to ASCE.

Figure 10 shows that the  $n_{ki}$  values are concentrated in the range of 1.4–1.7.

### 3.2. Investigation of Weak-Storey Irregularity

A total of 35 model buildings were identified for cases where there are two, three, four, five, and six spans and each span length ( $L_x$ ,  $L_y$ ) is 3, 3.5, 4, 4.5, 5, 5.5, and 6 m. The selected formwork plans are provided in Figure 11.

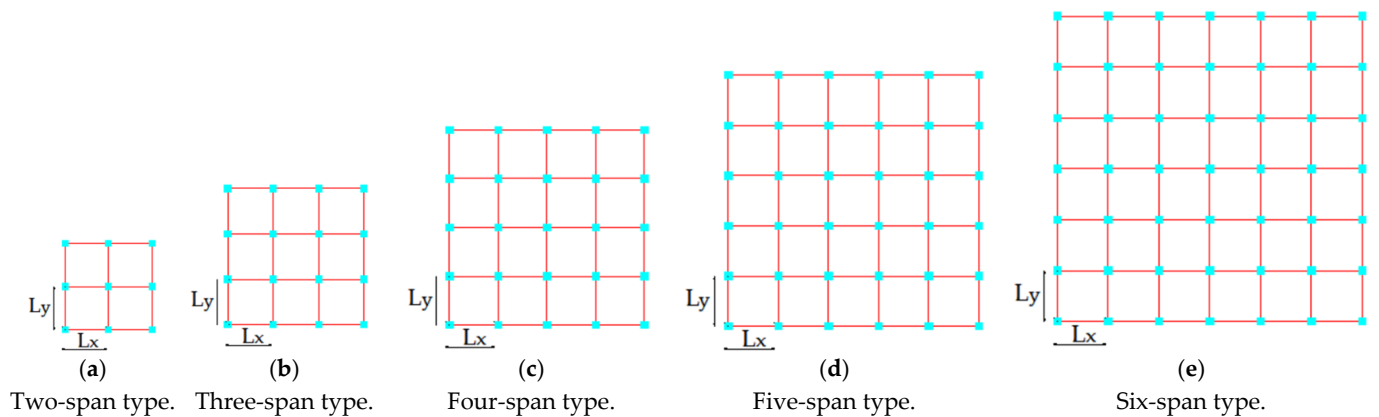


Figure 11. Two, three, four, five, and six-span formwork plans.

Since the ground floors of the model buildings are intended for commercial use or parking, the layout of the infill wall was made such that each building's ground floor has no infill walls in the x-direction (Type 1a wall layout), one of the exterior axes in the x-direction has an infill wall (Type 2a wall layout), and one of the exterior and interior axes in the x-direction has an infill wall (Type 3a wall layout). All the axes of the upper floors have infill walls. As an example, the infill wall layout of the ground and upper floors of a four-span model building is provided in Figure 12.

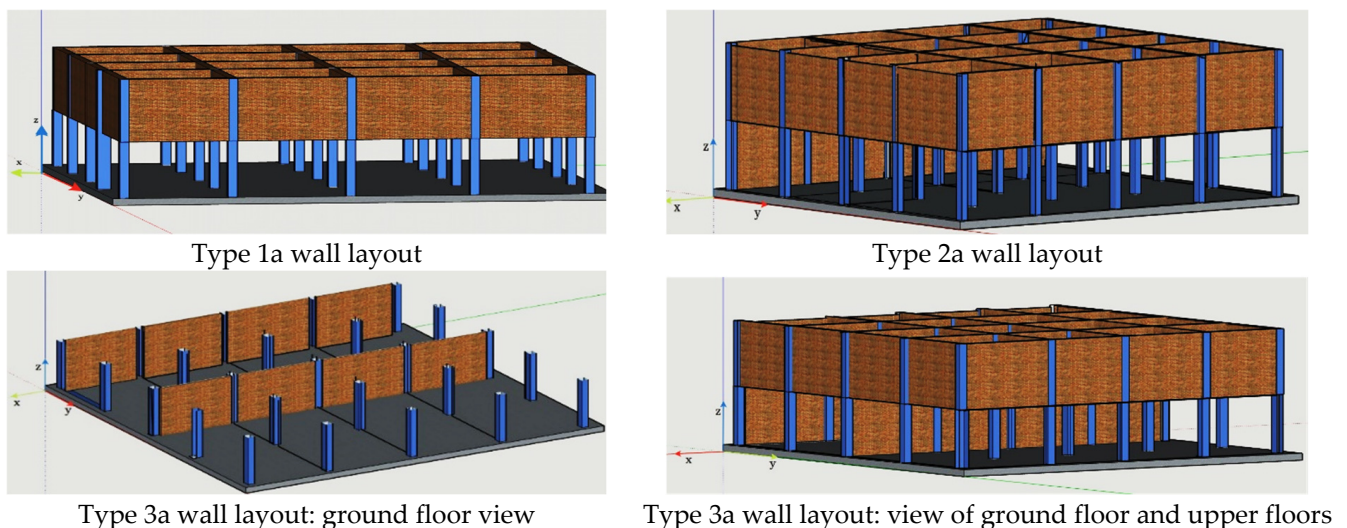
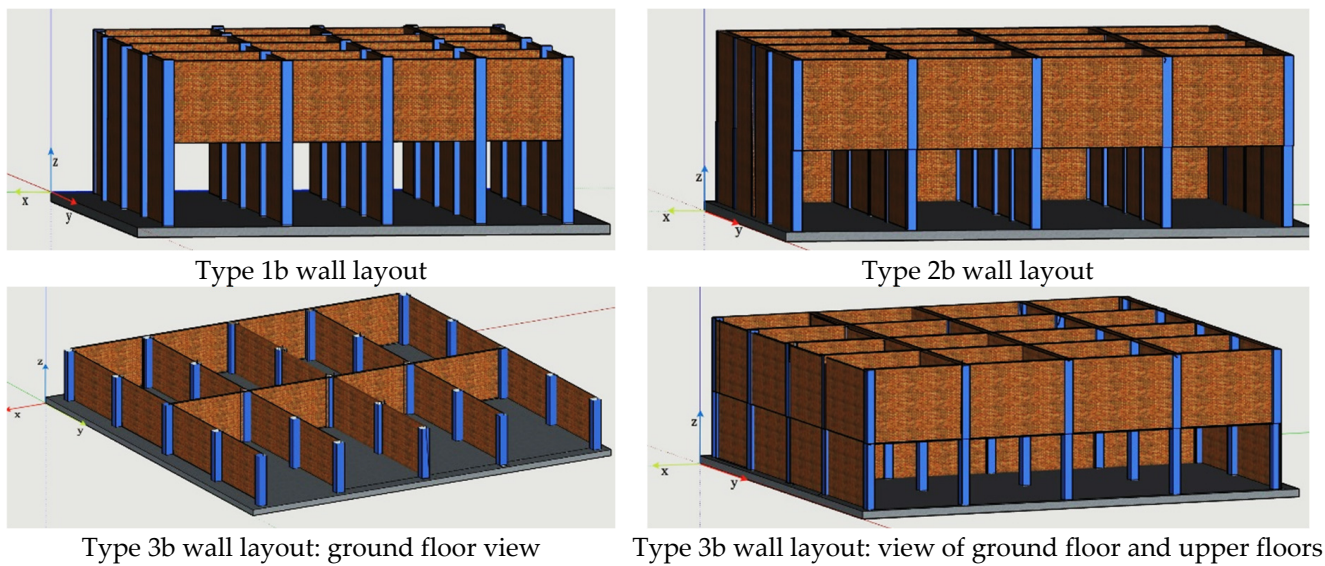


Figure 12. Infill wall layout in the x-direction for the ground floor and upper floors of a 4-span model building.

Examining the weak-storey irregularity scenarios for the x-direction of the model buildings is sufficient. Because the presence of weak-storey irregularity in only one direction of the building will cause weak-storey formation in the building. As the presence of infill walls in the y-direction of the ground floor does not change the effective shear area of the x-direction, the Type 1a wall layout will yield the same results as the Type 1b wall layout, Type 2a will be the same as Type 2b, and Type 3a will be the same as Type 3b. The Type 1b,

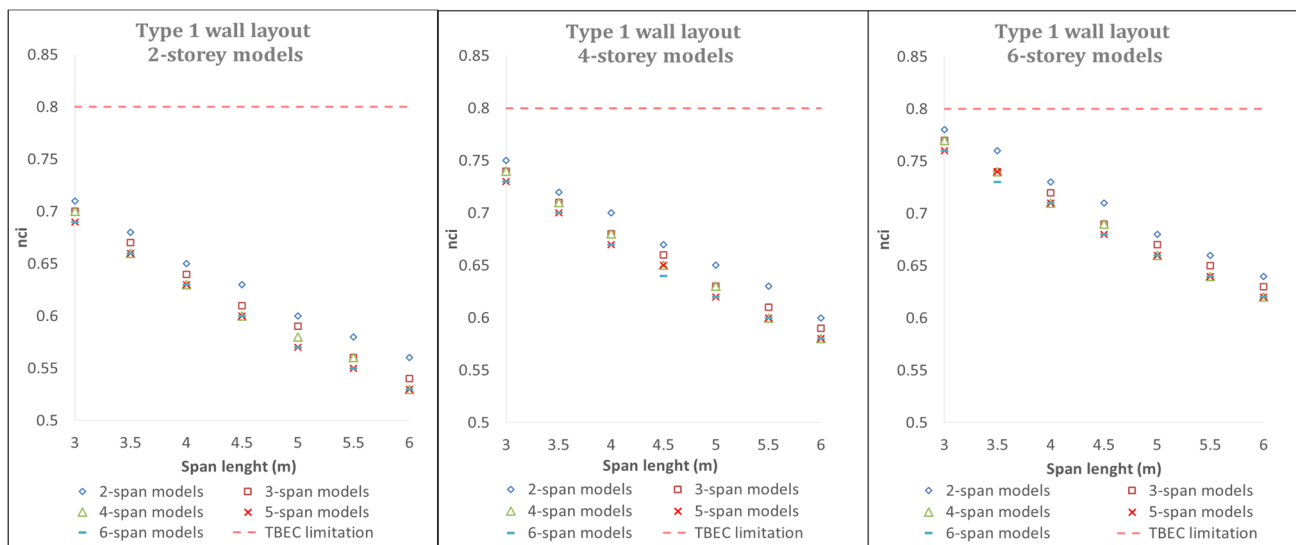
Type 2b, and Type 3b wall layouts obtained by adding infill walls in the y-direction to the infill wall layouts in Figure 12 are given in Figure 13.



**Figure 13.** Infill wall layout in both the x- and y-directions for the ground floor and upper floors of a 4-span model building.

In this study, Type 1a and Type 1b will be referred to as Type 1, Type 2a and Type 2b as Type 2, and Type 3a and Type 3b as Type 3. In all of the models, brick infill walls with infill wall thicknesses on the exterior axes are taken to be 20 cm thick and those on the interior axes as 14 cm. Each of the 35 model buildings has been modelled to have two, four, and six storeys. In the six-storey buildings, the column sections are  $65 \times 30$  cm; in the four-storey buildings, they are  $55 \times 30$  cm; and in the two-storey buildings, they are  $45 \times 30$  cm.

The weak-storey irregularity coefficients ( $n_{ci}$ ) for each of the different cases of infill wall layout, number of spans, span length, and number of storeys were obtained according to the TBEC (Figure 14).



(a)

**Figure 14.** Cont.

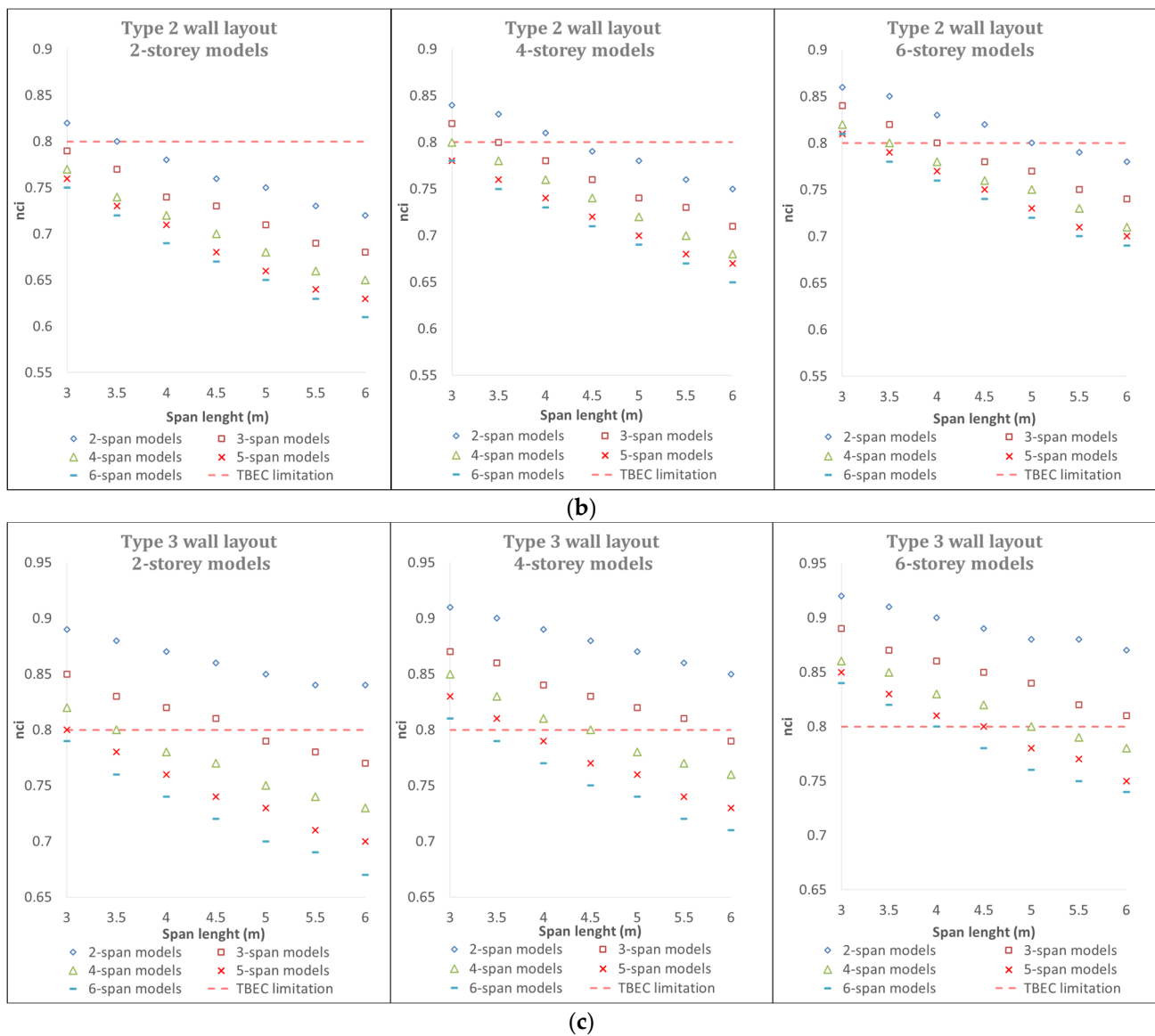


**Figure 14.** (a) Weak-storey irregularity coefficients obtained for Type 1 infill wall layout. (b) Weak-storey irregularity coefficients obtained for Type 2 infill wall layout. (c) Weak-storey irregularity coefficients obtained for Type 3 infill wall layout.

Figure 14 shows that the Type 1 infill wall layout causes weak-storey irregularity in all of the models. The Type 2 infill wall layout has caused weak-storey irregularity in 66% of the six-storey models, 83% of the four-storey models, and 94% of the two-storey models. The Type 3 infill wall layout has led to weak-storey irregularity in 26% of the six-storey models, 43% of the four-storey models, and 60% of the two-storey models. It is observed that as the number of spans or the span length increases in all models, and the weak-storey irregularity coefficient decreases. As the number of storeys increases, the column cross-sectional dimensions also increase; thus, the ratio of the column effective cross-sectional area  $(\sum A_w)_i$  in the total effective shear area  $(\sum A_e)_i$  increases, and consequently, the effect of the amount of infill walls on the weak storey irregularity decreases. Therefore, it can be said that the effect of the amount of infill walls on weak-storey irregularity is higher in low-rise buildings compared to mid-rise buildings. The results in Figure 14 show that structures without infill walls in one direction or with infill walls in only one of the outer axes in one direction are very sensitive to weak story formation.

According to ASCE, the amount of infill wall does not affect the weak-storey irregularity. Weak-storey irregularity usually occurs in buildings with vertical discontinuities or where the cross-sectional dimensions of load-bearing elements are reduced.

#### 4. Conclusions and Discussion

In this study, 96 model buildings were designed to investigate the reasons for soft-storey formation in buildings, and the ground floor heights causing soft-storey irregularity in each of these models were calculated according to the TBEC and ASCE regulations. In addition, 105 model buildings were designed to investigate the weak-storey formation, and the weak-storey irregularity coefficients for each of these models were calculated according to the TBEC. The findings obtained from the study are summarized below:

- (a) According to the formulas given in the TBEC, the ground floor heights ( $h_{gf}$ ) that cause soft-storey irregularities are too high to be used in practice, especially in buildings above three storeys (this can be seen in Figure 6). The results reveal that, even if the buildings are designed with very high ground floor heights, they do not have soft-storey irregularities according to the formulas given in the TBEC, but they can be damaged by earthquake effects due to soft-storey formation. This can be attributed to the excessively high limit value of the soft-storey irregularity coefficient ( $n_{ki} > 2$ ) in the TBEC.
- (b) According to the ASCE, the ground floor heights ( $h_{gf}$ ) that cause soft-storey irregularity are the ground floor heights that can be seen in practice. Therefore, based on the ASCE results, the soft-storey irregularity coefficients of each model building examined within the scope of the study were recalculated according to the TBEC, and it was determined that these values were concentrated in the range of 1.4–1.7. Updating the soft-storey irregularity coefficient limit value to 1.4 instead of 2 in the TBEC will prevent the design of buildings with very high ground floor heights and will keep the buildings on the safer side.
- (c) According to the TBEC, as the number of storeys increases, the ground floor heights that cause soft-storey irregularity rise in an exaggerated manner. In some models, the presence of a mezzanine floor in the building reduced the soft-storey risk. In addition, there are significant differences between the results obtained with the TBEC and the ASCE regulations (ground floor heights causing soft-storey irregularity). In fact, in some models, the differences between the regulations have reached up to 167%. It can be concluded from these results that the soft-storey irregularity formulas in the TBEC regulation should be discussed.
- (d) The fact that the ground floor is higher than the other floors causes this floor to be more flexible. Therefore, the relative storey drift of the ground floor under the effects of an earthquake is higher than that of the upper floors. However, according to the soft-storey irregularity coefficient ( $n_{ki}$ ) formula in the TBEC (Equation (1)), soft-storey irregularity is checked by dividing the relative drifts ( $\Delta_i$ ) by the storey height ( $h_i$ ); that is, by looking at the ( $\Delta_i/h_i$ ) ratio between the storeys. Increasing the relative storey drifts and ground floor height together does not change the ( $\Delta_i/h_i$ ) ratio much for the ground floor. However, when the ground floor height has very high values, since the relative drifts increase excessively, the coefficient of soft-storey irregularity ( $n_{ki}$ ) exceeds 2, and soft-storey irregularity occurs in the building. As a result, the ground floor heights that will cause soft-storey formation in the building are too large to be seen in practice. Since the height of the ground floor directly affects the stiffness in the soft-storey irregularity formulas in the ASCE, the increase in the height of the ground floor immediately affects the results, which provides more conservative results.
- (e) In some buildings in Türkiye where the ground floor is used for commercial purposes or as a parking lot, infill walls are not used on the interior axes for a more efficient use of interior space, or infill walls are not used on the exterior axes for a more efficient commercial use of building facades. The study revealed that the risk of weak-storey

irregularity is high in buildings with no infill walls in one direction or with infill walls in only one of the exterior axes in one direction.

This study was conducted on weak- and soft-storey formations, which are one of the main causes of earthquake damage to buildings in Türkiye. It is worth noting that code recommendations also use capacity design principles and drift (both inter-storey and roof drift) limitations, which limit the irregularities, especially those related to members, and hence, the structural capacities. Accordingly, the use of only soft-storey irregularity calculations is not adequate to come to a conclusion and question the irregularity of seismic codes. In future studies, it is thought that investigating other factors that cause earthquake damage to buildings and comparing the irregularity conditions and formulas in the TBEC with the regulations of other countries will positively contribute to building regular buildings in Türkiye that can withstand earthquakes. The author is conducting ongoing studies and has future plans to investigate the effects of the results of the models in the study on effective relative storey drifts, relative storey drifts, and roof storey drifts using nonlinear static or dynamic methods.

**Funding:** This research received no external funding.

**Data Availability Statement:** Most data are included in the manuscript.

**Acknowledgments:** Thanks to the reviewers for their careful reading of the article, critical review, suggestions and very helpful comments.

**Conflicts of Interest:** The authors declare no conflict of interest.

## References

1. Barka, A.A.; Kadinsky-Cade, K. Strike-slip Fault Geometry in Turkey and Its Influence on Earthquake Activity. *Tectonics* **1988**, *7*, 663–684. [\[CrossRef\]](#)
2. Zengin, B.; Aydın, F. The Effect of Material Quality on Buildings Moderately and Heavily Damaged by the Kahramanmaraş Earthquakes. *Appl. Sci.* **2023**, *13*, 10668. [\[CrossRef\]](#)
3. Caglar, N.; Vural, I.; Kirtel, O.; Saribiyik, A.; Sumer, Y. Structural Damages Observed in Buildings after the January 24, 2020 Elazığ-Sivrice Earthquake in Türkiye. *Case Stud. Constr. Mater.* **2023**, *18*, e01886. [\[CrossRef\]](#)
4. İnce, O. Structural Damage Assessment of Reinforced Concrete Buildings in Adiyaman after Kahramanmaraş (Türkiye) Earthquakes on 6 February 2023. *Eng. Fail. Anal.* **2024**, *156*, 107799. [\[CrossRef\]](#)
5. Yön, B. Identification of Failure Mechanisms in Existing Unreinforced Masonry Buildings in Rural Areas after April 4, 2019 Earthquake in Turkey. *J. Build. Eng.* **2021**, *43*, 102586. [\[CrossRef\]](#)
6. Doğangün, A.; Yön, B.; Onat, O.; Emin Öncü, M.; Sağlıroğlu, S. Seismicity of East Anatolian of Turkey and Failures of Infill Walls Induced by Major Earthquakes. *J. Earthq. Tsunami* **2021**, *15*, 2150017. [\[CrossRef\]](#)
7. Sayin, E.; Yön, B.; Calayir, Y.; Karaton, M. Failures of Masonry and Adobe Buildings during the June 23, 2011 Maden-(Elazığ) Earthquake in Turkey. *Eng. Fail. Anal.* **2013**, *34*, 779–791. [\[CrossRef\]](#)
8. Doğangün, A. Performance of Reinforced Concrete Buildings during the May 1, 2003 Bingöl Earthquake in Turkey. *Eng. Struct.* **2004**, *26*, 841–856. [\[CrossRef\]](#)
9. AFAD. *Turkish Ministry of Interior Disaster and Emergency Management Presidency*; Turkish Ministry of Interior: Ankara, Türkiye, 2023.
10. Ivanov, M.L.; Chow, W.K. Structural Damage Observed in Reinforced Concrete Buildings in Adiyaman during the 2023 Türkiye Kahramanmaraş Earthquakes. *Structures* **2023**, *58*, 105578. [\[CrossRef\]](#)
11. Scawthorn, C.; Johnson, G.S. Preliminary Report: Kocaeli (Izmit) Earthquake of 17 August 1999. *Eng. Struct.* **2000**, *22*, 727–745. [\[CrossRef\]](#)
12. Akkar, S.; Boore, D.M.; Gülkan, P. An Evaluation of the Strong Ground Motion Recorded during the May 1, 2003 Bingöl Turkey, Earthquake. *J. Earthq. Eng.* **2005**, *9*, 173–197. [\[CrossRef\]](#)
13. Gur, T.; Pay, A.C.; Ramirez, J.A.; Sozen, M.A.; Johnson, A.M.; Irfanoglu, A.; Bobet, A. Performance of School Buildings in Turkey during the 1999 Düzce and the 2003 Bingöl Earthquakes. *Earthq. Spectra* **2009**, *25*, 239–256. [\[CrossRef\]](#)
14. Inel, M.; Ozmen, H.B.; Cayci, B.T. Evaluation of Reasons of the Damages after Simav and Van (2011) Earthquakes. *Pamukkale Univ. J. Eng. Sci.* **2013**, *19*, 256–265. [\[CrossRef\]](#)
15. Muvafik, M. Field Investigation and Seismic Analysis of a Historical Brick Masonry Minaret Damaged during the Van Earthquakes in 2011. *Earthq. Struct.* **2014**, *6*, 457–472. [\[CrossRef\]](#)
16. Sayin, E.; Yon, B.; Calayir, Y.; Gor, M. Construction Failures of Masonry and Adobe Buildings during the 2011 Van Earthquakes in Turkey. *Struct. Eng. Mech.* **2014**, *51*, 503–518. [\[CrossRef\]](#)
17. Baran, E.; Mertol, H.C.; Gunes, B. Damage in Reinforced-Concrete Buildings during the 2011 Van, Turkey, Earthquakes. *J. Perform. Constr. Facil.* **2014**, *28*, 466–479. [\[CrossRef\]](#)

18. Bayraktar, A.; Altunışık, A.C.; Türker, T.; Karadeniz, H.; Erdogdu, S.; Angin, Z.; Özşahin, T.S. Structural Performance Evaluation of 90 RC Buildings Collapsed during the 2011 Van, Turkey, Earthquakes. *J. Perform. Constr. Facil.* **2015**, *29*, 4014177. [[CrossRef](#)]
19. Murat, O. Field Reconnaissance of the October 23, 2011, Van, Turkey, Earthquake: Lessons from Structural Damages. *J. Perform. Constr. Facil.* **2015**, *29*, 4014125. [[CrossRef](#)]
20. Korkmaz, S.Z. Observations on the Van Earthquake and Structural Failures. *J. Perform. Constr. Facil.* **2015**, *29*, 4014033. [[CrossRef](#)]
21. Karataş, L.; Bayhan, B. Damage Assessment and Restoration Proposal Following the 2023 Türkiye Earthquakes: UNESCO World Heritage Site Diyarbakır City Walls, Türkiye. *Herit. Sci.* **2023**, *11*, 228. [[CrossRef](#)]
22. Bekdaş, G.; Sayin, B.; Çelik Sola, Ö.; Güner, A. Assessment of the Material Quality of Damaged Structures after Earthquake in Van, Turkey. *J. Mater. Civ. Eng.* **2016**, *28*, 4016110. [[CrossRef](#)]
23. Güney, D.; Kuruşçu, A.O.; Arun, G. Damage Evaluation of Masonry Buildings after Van Earthquakes in 2011. *Int. J. Archit. Herit.* **2016**, *10*, 269–280.
24. Erdil, B. Why RC Buildings Failed in the 2011 Van, Turkey, Earthquakes: Construction versus Design Practices. *J. Perform. Constr. Facil.* **2017**, *31*, 4016110. [[CrossRef](#)]
25. Oyguc, R.; Oyguc, E. 2011 Van Earthquakes: Lessons from Damaged Masonry Structures. *J. Perform. Constr. Facil.* **2017**, *31*, 4017062. [[CrossRef](#)]
26. Atmaca, B.; Demir, S.; Günaydin, M.; Altunışık, A.C.; Hüsem, M.; Ateş, Ş.; Adanur, S.; Angin, Z. Field Investigation on the Performance of Mosques and Minarets during the Elazığ-Sivrice Earthquake. *J. Perform. Constr. Facil.* **2020**, *34*, 4020120. [[CrossRef](#)]
27. Cenan Mertol, H.; Tunc, G.; Akis, T. Damage Observation of Reinforced Concrete Buildings after 2020 Sivrice (Elazığ) Earthquake, Turkey. *J. Perform. Constr. Facil.* **2021**, *35*, 4021053. [[CrossRef](#)]
28. Wang, T.; Chen, J.; Zhou, Y.; Wang, X.; Lin, X.; Wang, X.; Shang, Q. Preliminary Investigation of Building Damage in Hatay under February 6, 2023 Turkey Earthquakes. *Earthq. Eng. Eng. Vib.* **2023**, *22*, 853–866. [[CrossRef](#)]
29. Onat, O.; Deniz, F.; Özmen, A.; Özdemir, E.; Sayın, E. Performance Evaluation and Damage Assessment of Historical Yusuf Ziya Pasha Mosque after February 6, 2023 Kahramanmaraş Earthquakes. *Structures* **2023**, *58*, 105415. [[CrossRef](#)]
30. Binici, B.; Yakut, A.; Kadas, K.; Demirel, O.; Akpınar, U.; Canbolat, A.; Yurtseven, F.; Oztaskin, O.; Aktas, S.; Canbay, E. Performance of RC Buildings after Kahramanmaraş Earthquakes: Lessons toward Performance Based Design. *Earthq. Eng. Eng. Vib.* **2023**, *22*, 883–894. [[CrossRef](#)]
31. Gurbuz, T.; Cengiz, A.; Kolemenoglu, S.; Demir, C.; Ilki, A. Damages and Failures of Structures in İzmir (Turkey) during the October 30, 2020 Aegean Sea Earthquake. *J. Earthq. Eng.* **2023**, *27*, 1565–1606. [[CrossRef](#)]
32. Işık, E.; Büyüksaraç, A.; Avcil, F.; Arkan, E.; Aydın, M.C.; Ulu, A.E. Damage Evaluation of Masonry Buildings during Kahramanmaraş (Türkiye) Earthquakes on February 06, 2023. *Earthq. Struct.* **2023**, *25*, 209–221. [[CrossRef](#)]
33. Mertol, H.C.; Tunç, G.; Akış, T.; Kantekin, Y.; Aydın, İ.C. Investigation of RC Buildings after 6 February 2023, Kahramanmaraş, Türkiye Earthquakes. *Buildings* **2023**, *13*, 1789. [[CrossRef](#)]
34. Balun, B. Assessment of Seismic Parameters for 6 February 2023 Kahramanmaraş Earthquakes. *Struct. Eng. Mech.* **2023**, *88*, 117–128. [[CrossRef](#)]
35. Altunışık, A.; Arslan, M.; Kahya, V.; Aslan, B.; Sezdirmez, T.; Dok, G.; Kirtel, O.; Öztürk, H.; Sunca, F.; Baltacı, A. Field Observations and Damage Evaluation in Reinforced Concrete Buildings After the February 6th, 2023, Kahramanmaraş-Türkiye Earthquakes. *J. Earthq. Tsunami* **2023**, *17*, 2350024. [[CrossRef](#)]
36. Kazaz, İ.; Bilge, İ.H.; Gürbüz, M. Near-Fault Ground Motion Characteristics and Its Effects on a Collapsed Reinforced Concrete Structure in Hatay during the February 6, 2023 Mw7.8 Kahramanmaraş Earthquake. *Eng. Struct.* **2024**, *298*, 117067. [[CrossRef](#)]
37. Işık, E. Structural Failures of Adobe Buildings during the February 2023 Kahramanmaraş (Türkiye) Earthquakes. *Appl. Sci.* **2023**, *13*, 8937. [[CrossRef](#)]
38. Ozturk, M.; Arslan, M.H.; Dogan, G.; Ecemis, A.S.; Arslan, H.D. School Buildings Performance in 7.7 Mw and 7.6 Mw Catastrophic Earthquakes in Southeast of Turkey. *J. Build. Eng.* **2023**, *79*, 107810. [[CrossRef](#)]
39. Bayraktar, A.; Altunışık, A.C.; Pehlivan, M. Performance and Damages of Reinforced Concrete Buildings during the October 23 and November 9, 2011 Van, Turkey, Earthquakes. *Soil Dyn. Earthq. Eng.* **2013**, *53*, 49–72. [[CrossRef](#)]
40. Jara, J.M.; Hernández, E.J.; Olmos, B.A.; Martínez, G. Building Damages during the September 19, 2017 Earthquake in Mexico City and Seismic Retrofitting of Existing First Soft-Story Buildings. *Eng. Struct.* **2020**, *209*, 109977. [[CrossRef](#)]
41. Kirac, N.; Dogan, M.; Ozbasaran, H. Failure of Weak-Storey during Earthquakes. *Eng. Fail. Anal.* **2011**, *18*, 572–581. [[CrossRef](#)]
42. Işık, E.; Avcil, F.; Büyüksaraç, A.; İzol, R.; Hakan Arslan, M.; Aksoylu, C.; Harirchian, E.; Eysüren, O.; Arkan, E.; Şakir Güngür, M.; et al. Structural Damages in Masonry Buildings in Adıyaman during the Kahramanmaraş (Türkiye) Earthquakes (Mw 7.7 and Mw 7.6) on 06 February 2023. *Eng. Fail. Anal.* **2023**, *151*, 107405. [[CrossRef](#)]
43. Nuhoglu, A.; Erener, M.F.; Hızal, Ç.; Kınçal, C.; Erdoğan, D.Ş.; Özdağ, Ö.C.; Akgün, M.; Ercan, E.; Kalfa, E.; Köksal, D.; et al. A Reconnaissance Study in İzmir (Bornova Plain) Affected by October 30, 2020 Samos Earthquake. *Int. J. Disaster Risk Reduct.* **2021**, *63*, 102465. [[CrossRef](#)]
44. Qu, Z.; Zhu, B.; Cao, Y.; Fu, H. Rapid Report of Seismic Damage to Buildings in the 2022 M 6.8 Luding Earthquake, China. *Earthq. Res. Adv.* **2023**, *3*, 100180. [[CrossRef](#)]
45. Sezen, H.; Whittaker, A.S.; Elwood, K.J.; Mosalam, K.M. Performance of Reinforced Concrete Buildings during the August 17, 1999 Kocaeli, Turkey Earthquake, and Seismic Design and Construction Practise in Turkey. *Eng. Struct.* **2003**, *25*, 103–114. [[CrossRef](#)]

46. Ates, S.; Kahya, V.; Yurdakul, M.; Adanur, S. Damages on Reinforced Concrete Buildings Due to Consecutive Earthquakes in Van. *Soil Dyn. Earthq. Eng.* **2013**, *53*, 109–118. [[CrossRef](#)]
47. Doğan, M.; Kirac, N.; Gönen, H. Soft-Storey Behaviour in An Earthquake and Samples of Izmit-Duzce. In Proceedings of the Uluslararası Yapı ve Deprem Mühendisliği Sempozyumu, Orta Doğu Teknik Üniversitesi, Ankara, Turkey, 14 October 2002; pp. 42–49.
48. Dogan, M. Failure of Structural (RC, Masonry, Bridge) to Van Earthquake. *Eng. Fail. Anal.* **2013**, *35*, 489–498. [[CrossRef](#)]
49. Şahin, H.; Alyamaç, K.E.; Durucan, A.R.; Demirel, B.; Açıkgenç Ulaş, M.; Bildik, A.T.; Durucan, C.; Demir, T.; Ulucan, M.; Demirbaş, N. *January 24, 2020 Mw 6.8 Sivrice/Elazığ Earthquake Elazığ Region Structural Damages Investigation and Analysis Report*; Report No: 2020/D001; Construction and Concrete Application and Research Center, Fırat University: Elazığ, Türkiye, 2020.
50. Yakut, A.; Sucuoğlu, H.; Binici, B.; Canbay, E.; Donmez, C.; İlki, A.; Caner, A.; Celik, O.C.; Ay, B.Ö. Performance of Structures in İzmir after the Samos Island Earthquake. *Bull. Earthq. Eng.* **2022**, *20*, 7793–7818. [[CrossRef](#)]
51. Avcil, F.; Işık, E.; İzol, R.; Büyüksaraç, A.; Arkan, E.; Arslan, M.H.; Aksoyulu, C.; Eyisüren, O.; Harirchian, E. Effects of the February 6, 2023, Kahramanmaraş Earthquake on Structures in Kahramanmaraş City. *Nat. Hazards* **2023**, *120*, 2953–2991. [[CrossRef](#)]
52. Ozturk, M.; Arslan, M.H.; Korkmaz, H.H. Effect on RC Buildings of 6 February 2023 Turkey Earthquake Doublets and New Doctrines for Seismic Design. *Eng. Fail. Anal.* **2023**, *153*, 107521. [[CrossRef](#)]
53. Ruiz-García, J.; Cárdenas, Y. Seismic Performance Assessment of Weak First-Storey RC Buildings Designed with Old and New Seismic Provisions for Mexico City. *Eng. Struct.* **2021**, *232*, 111803. [[CrossRef](#)]
54. Guerrero, H.; Teran-Gilmore, A.; Zamora, E.; Escobar, J.A.; Gómez, R. Hybrid Simulation Tests of a Soft Storey Frame Building Upgraded with a Buckling-Restrained Brace (BRB). *Exp. Tech.* **2020**, *44*, 553–572. [[CrossRef](#)]
55. Jara, J.M.; Florio, E.; Olmos, B.A. Seismic Evaluation and Reliability Index of Soft Story Buildings on Flexible Soils by Using Old and Current Seismic Regulations in Mexico. *Eng. Struct.* **2023**, *286*, 116048. [[CrossRef](#)]
56. TBEC. *Turkey Building Earthquake Code*, Republic of Turkey Ministry of Interior Disaster and Emergency Management Authority; TBEC: Ankara, Turkey, 2018.
57. ASCE. *Minimum Design Loads for Buildings and Other Structures*; ASCE/SEI 7-22; ASCE: Reston, VA, USA, 2022.
58. Ulutas, H.; Koyuncu, E. Bant Pencere Kaynaklı Kısa Kolon Oluşumunun Yumuşak Kat Düzensizliği Üzerindeki Etkisinin İncelenmesi. In Proceedings of the 10th International Congress on Engineering, Architecture and Design, Istanbul, Turkey, 23–24 November 2022; pp. 329–335.

**Disclaimer/Publisher’s Note:** The statements, opinions and data contained in all publications are solely those of the individual author(s) and contributor(s) and not of MDPI and/or the editor(s). MDPI and/or the editor(s) disclaim responsibility for any injury to people or property resulting from any ideas, methods, instructions or products referred to in the content.